Original article

Structure and Climatic Intra-Annual Variability of Water Mass Characteristics in the Powell Basin and on the Adjacent Antarctic Peninsula Shelf

Yu. V. Artamonov, E. A. Skripaleva *, N. V. Nikolskii

Marine Hydrophysical Institute of RAS, Sevastopol, Russia
** e-mail: sea-ant@yandex.ru*

Abstract

The paper analyzes the long-term average structure and climatic intra-annual variability of water mass characteristics in the Powell Basin and adjacent water areas based on monthly average potential temperature and salinity data for each year from 1958 to 2021 from *ECMWF ORA-S*5 reanalysis. It is shown that the Antarctic Shelf Water is observed not only over the shallow shelf of the Joinville Archipelago, but also over the continental slope in the northwestern Weddell Sea. It is revealed that the layer of Circumpolar Deep Water is divided into Upper and Lower modifications. The Deep and Bottom Waters of the Weddell Sea do not appear as separate extremes on the long-term average θ,*S*-curves. It is shown that in the center of the cyclonic gyre in the Powell Basin, the Antarctic Winter Water core is located in a layer of 25–55 m. In the Scotia Sea, the Hesperides Trough, and over the Philip Ridge, the Antarctic Winter Water core deepens to 60–85 m. The minimum depths of the cores of the Upper and Lower modifications of the Circumpolar Deep Water (250–300 m and 500–600 m, respectively) are observed in the central part of the Powell Basin and closer to the center of the Weddell Sea Gyre, the maximum depths (1000–1300 m and 1100–1500 m, respectively) are observed over the slopes of the depths of the Joinville shelf and the South Scotia, Philip, and Joinville Ridges. It is shown that seasonal changes in the θ-index of the Antarctic Surface Water are maximum (3.5–4°C) in the southern Scotia Sea and in the Hesperides Trough. Seasonal changes in the *S*-index are maximum (1.8–1.9 PSU) over the Philip Ridge and in the northern and southern parts of the Powell Basin. Intra-annual changes in the θ,*S*-indices of the Antarctic Shelf Water reach 1.6–1.8 °C and 1.5 PSU, respectively. The Weddell Sea Surface Water is characterized by weak changes in the θ-index, while changes in its *S*-index reach almost 1.8 PSU. Intra-annual changes in the θ,*S*-indices of Antarctic Winter Water are maximum in the central part of the Powell Basin (up to 1 °C and 1.1 PSU).

Keywords: Southern Ocean, Weddell Sea, Powell Basin, Antarctic shelf, water masses, potential water temperature, salinity, neutral density, spatiotemporal variability, vertical water structure

Acknowledgments: The work was carried out under FSBSI FRC MHI state assignment FNNN-2021-0004 «Fundamental studies of oceanological processes which determine the state and evolution of the marine environment influenced by natural and anthropogenic factors, based on observation and modeling methods» («Oceanological processes» code).

For citation: Artamonov, Yu.V., Skripaleva, E.A. and Nikolskii, N.V., 2023. Structure and Climatic Intra-Annual Variability of Water Mass Characteristics in the Powell Basin and on the Adjacent Antarctic Peninsula Shelf. *Ecological Safety of Coastal and Shelf Zones of Sea*, (3), pp. 22–39.

Структура и климатическая внутригодовая изменчивость характеристик водных масс в котловине Пауэлл и на прилегающем шельфе Антарктического полуострова

Ю. В. Артамонов, Е. А. Скрипалева *, Н. В. Никольский

Морской гидрофизический институт РАН, Севастополь, Россия
** e-mail: sea-ant@yandex.ru*

Аннотация

По среднемесячным значениям потенциальной температуры и солености для каждого года с 1958 по 2021 г. из реанализа *ECMWF ORA-S*5 проанализированы среднемноголетняя структура и климатическая внутригодовая изменчивость характеристик водных масс котловины Пауэлл и прилегающих акваторий. Показано, что антарктическая шельфовая вода наблюдается не только над мелководным шельфом архипелага Жуэнвиль, но и над свалом глубин в северо-западной части моря Уэдделла. Выявлено, что слой циркумполярной глубинной воды разделяется на верхнюю и нижнюю модификации. Глубинная и донная воды моря Уэдделла в виде отдельных экстремумов на среднемноголетних θ,*S*-кривых не проявляются. Показано, что в центре циклонического круговорота в котловине Пауэлл ядро антарктической зимней воды располагается в слое 25–55 м. В море Скоша, желобе Гесперид и над хребтом Филипп оно заглубляется до 60–85 м. Минимальные глубины залегания ядер верхней и нижней модификаций циркумполярной глубинной воды (соответственно 250–300 и 500–600 м) наблюдаются в центральной части котловины Пауэлл и ближе к центру круговорота моря Уэдделла, максимальные глубины (соответственно 1000–1300 и 1100–1500 м) – над свалами глубин шельфа Жуэнвиль и хребтов Южный Скоша, Филипп и Жуэнвиль. Показано, что сезонные изменения θ-индекса антарктической поверхностной воды максимальны (3.5–4 °С) в южной части моря Скоша и в желобе Гесперид, *S*-индекса (1.8–1.9 ЕПС) – над хребтом Филипп и в северной и южной частях котловины Пауэлл. Внутригодовые изменения θ,*S*-индексов антарктической шельфовой воды достигают 1.6–1.8 °С и 1.5 ЕПС соответственно. Поверхностная вода моря Уэдделла характеризуется слабыми изменениями θ-индекса, тогда как изменения ее *S*- индекса достигают почти 1.8 ЕПС. Внутригодовые изменения θ,*S*-индексов антарктической зимней воды максимальны в центральной части котловины Пауэлл (до 1 °С и 1.1 ЕПС).

Ключевые слова: Южный океан, море Уэдделла, котловина Пауэлл, антарктический шельф, водные массы, потенциальная температура морской воды, соленость, нейтральная плотность, пространственно-временная изменчивость, вертикальная структура вод

Благодарности: работа выполнена в рамках государственного задания ФГБУН ФИЦ МГИ по теме FNNN-2021-0004 «Фундаментальные исследования океанологических процессов, определяющих состояние и эволюцию морской среды под влиянием естественных и антропогенных факторов, на основе методов наблюдения и моделирования» (шифр «Океанологические процессы»).

Для цитирования: *Артамонов Ю. В., Скрипалева Е. А., Никольский Н. В.* Структура и климатическая внутригодовая изменчивость характеристик водных масс в котловине Пауэлл и на прилегающем шельфе Антарктического полуострова // Экологическая безопасность прибрежной и шельфовой зон моря. 2023. № 3. С. 22–39. EDN ZDFRLB.

Introduction

Water masses and their boundaries (hydrological fronts) are the most important abiotic factors that determine the level of bioproductivity of water, influencing the spatial distribution of nutrients [1–7]. The most bioproductive area is the southwestern part of the Southern Ocean Atlantic sector, where the Antarctic krill spawn on the vast Antarctic Peninsula shelf. The krill transported from spawning grounds along the western periphery of the Weddell Sea Gyre (WSG) accumulate in the Powell Basin [8–10]. Further, the main transfer of the krill aggregations occurs along the northern periphery of the WSG, passing along the Philip and South Scotia Ridges that bound the Powell Basin from the north [2, 3, 5]. The commercial significance of the shelf areas of the Antarctic Peninsula, the northwestern Weddell Sea, and the Powell Basin led to the appearance of a number of works devoted to the study of the processes of formation, modification and distribution of water masses in this region [1)] [2, 10–21].

The research results show that, in general, the vertical structure of the local waters is characterized by the following features [1)] [1, 2, 11–14, 17–20].
In the upper layer, there are Antarctic Surface Waters (AASW) consisting of two modifications. They are relatively warm and desalinated well-mixed Summer Waters (AASSW) and colder and saltier Winter Waters (AASWW). Deeper down, there is a subsurface layer of the Antarctic Winter Water (AAWW) characterized by the minimum temperature and representing the remnants of the previous winter upper mixed layer of the AASWW. Below, a layer of circumpolar deep water (CDW) lies, which, to the south of the Antarctic Circumpolar Current (ACC) system, is called “warm deep water” (WDW) according to the terminology of some authors [12, 14, 15, 20]. In the upper part of the layer, the CDW is determined by the maximum temperature (Upper CDW), and at intermediate depths – by the maximum salinity (Lower CDW). It should be noted that some authors believe that in the WSG region, it is impossible to divide the CDW layer into Upper and Lower modifications [2]. Other authors [18] believe that to the south of the ACC system, the entire CDW layer is occupied by its Lower modification characterized by the maximum salinity.

[1)] Sarukhanyan, E.I. and Smirnov, N.P., 1986. [*Water Masses and Circulation of the South Ocean*]. Leningrad: Gidrometeoizdat, 288 p. (in Russian).

In [20], three modifications of the WDW with different thermohaline characteristics were identified in the Powell Basin: Upper, Middle, and Lower. Underneath the CDW layer, a layer of Weddell Sea Deep Water (WSDW) lies, under which a layer of Weddell Sea Bottom Water (WSBW) is located. The WSDW from the Powell Basin penetrates north into the Hesperides Trough and into the Scotia Sea through the deep-sea passages of the surrounding bottom uplifts [2, 15–18], while the WSBW does not spread beyond the WSG boundaries [17, 22].

The Antarctic Shelf Waters (AAShW) with temperatures close to the sea water freezing point are formed on the shallow shelves surrounding the Powell Basin as a result of powerful autumn-winter convection, leading to thermal uniformity throughout the entire layer, from the surface to the bottom. These waters are characterized by low salinity in summer when sea ice melts over the Antarctic shelf, and high salinity in winter when the sea ice is formed [1] [1, 2, 11–14, 17, 19, 20].

It should be noted that most studies that analyze the structure of water masses in the region under consideration are based on the data provided by irregular synoptic hydrological measurements, carried out due to severe weather conditions mainly in the warm period and not always coinciding in space. Analysis and identification of water masses based on data from scattered synoptic surveys at individual sections and hydrological stations lead to the fact that the amount of water masses does not coincide with their modifications in the works of various authors [2, 18, 20].

Currently, constant replenishment of factual databases and increase in the length of time series of remote measurements contribute to the introduction of modern versions of oceanic reanalyses, which assimilate all available data from contact and satellite measurements. The use of such reanalyses makes it possible to clarify the long-term average spatial structure of waters and provide estimates of intra-annual changes in the characteristics of water masses, which is necessary to interpret the structural features of waters obtained from the results of actual field measurements [9, 10, 19, 20, 23].

The purpose of this work is to use the *ECMWF ORA-S5* oceanic reanalysis data to analyze the long-term average spatial structure of water masses and study the climatic intra-annual variability of their characteristics in the Powell Basin and adjacent waters (the eastern shelf of the Antarctic Peninsula and the northwestern Weddell Sea).

Materials and methods

The research examines the region of the Southern Ocean east of the Antarctic Peninsula, located between 60° and 65° south and 56° and 47.5° west. It includes the shelf of the Joinville Archipelago, the Powell Basin, the northwestern Weddell Sea, and the southwestern Scotia Sea. The Powell Basin is separated from the main basin of the Weddell Sea by the Joinville Ridge, and from the Scotia Sea by the South Scotia and Philip Ridges (Fig. 1, *a*). When constructing the bottom topography diagram, the data from *General Bathymetric Chart of the Oceans* (*GEBCO*) (URL: http://www.gebco.net/data_and_products/gridded_bathymetry_data/) were used with a spatial resolution of 15 arcseconds.

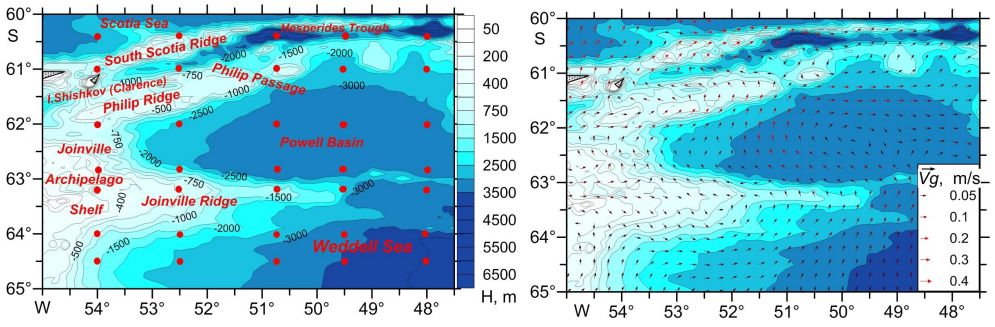

F i g . 1 . Study area (*a*) and distribution of long-term average vectors of geostrophic currents (*b*). The red dots show the grid nodes for which examples of θ,*S*-curves are presented in Fig. 3

Analysis of the thermohaline structure of waters and identification of water masses were carried out in accordance with *European Centre for Medium-Range Weather Forecasts OCEAN*5 *system* (*ECMWF ORAS*5) (URL: https://cds.climate.copernicus.eu/cdsapp#!/dataset/reanalysis-oras5?tab=form) reanalysis data. The reanalysis contains monthly averages of potential temperature θ (°C) and salinity *S* (PSU) at grid points of approximately 0.25° × 0.25° at 75 vertical levels in *sigma*-coordinates for each year within the period from 1958 to 2021. These values are derived from the *Nucleus for European Modelling of the Ocean* (*NEMO*) ocean model and the *NEMOVAR* ocean assimilation system adopting surface and subsurface temperature, salinity, sea ice concentration, and sea level anomalies [24]. Based on the initial data, long-term and climatic monthly average values of potential temperature and salinity were calculated. To identify the cores of water masses and their thermohaline indices, long-term and climatic monthly average θ,*S*-curves were constructed at each grid node. According to the classical *T*,*S*-analysis, the amount of water masses was determined on the θ,*S*-curve by the number of extrema plus two end points [2), 3)] [25]. To clarify the vertical structure of the waters, we analyzed the vertical distributions of neutral density γ^n (kg/m^3), which is a function of salinity, in situ temperature, pressure, longitude and latitude [26] and indirectly reflects the position of the boundaries of water masses. When assessing the seasonal variability of thermohaline indices of water masses, the spatial distributions of intra-annual root-mean-square deviations (RMSD) of temperature and salinity were analyzed.

The spatial distributions of water mass characteristics were interpreted against the background of the geostrophic circulation of water. The long-term

---

[2)] Mamayev, O.I., 1975. *Temperature-Salinity Analysis of World Ocean Waters*. Amsterdam: Elsevier Scientific Publishing, 374 p.

[3)] Bulgakov, N.P., 1975. [*Convection in the Ocean*]. Moscow: Nauka, 272 p. (in Russian).

average structure of currents was analyzed using the *Copernicus Marine Environment Monitoring Service* (*CMEMS*) (URL: http://marine.copernicus.eu/?option=com_csw&view=details&product_id=SEA-LEVEL_GLO_PHY_L4_REP_OBSERVATIONS_008_047) reanalysis data containing average daily values of geostrophic velocity components at regular grid nodes with a step of 0.25° from 1993 to 2020. These values were used when calculating the long-term average values of the velocity modulus $\vec{V}g$ and the direction of current vectors (Fig. 1, *b*).

Main results

Distributions of long-term average values of potential temperature and salinity on vertical meridional sections and long-term average θ,*S*-curves, examples of which are presented in Figs. 2 and 3, showed that the structure of waters in the studied water areas differing in orographic conditions also differentiates significantly.

In deep-water areas of the water area, such as the southern Scotia Sea, the Hesperides Trough, the Powell Basin, the northwestern Weddell Sea, adjacent to the Antarctic shelf, the Antarctic type of vertical water structure can be observed. In the distributions of temperature (Fig. 2, *a*, *c*, *e*) and long-term average θ,*S*-curves (Fig. 3) north of the shelf and the Joinville Ridge in a layer of approximately 25–150 m, subsurface minimum θ characterizing the Antarctic Winter Water is clearly visible. Temperature values in the Antarctic Winter Water layer decrease significantly in the deep-sea areas between the South Scotia and Philip Ridges and over the slopes of the depths of the Joinville Ridge (θ < −1.5 °C) and increase (θ < −1 °C) in the Scotia Sea, Hesperides Trough, and central part of the Powell Basin (Figs. 2, *a*, *c*, *e*; 3). The distribution of neutral density isolines γ^n shows that isopycnic line 27.95 can be conventionally taken as the lower boundary of the Antarctic Winter Water. In the open Weddell Sea, the subsurface minimum corresponding to the Antarctic Winter Water is not observed in the long-term average temperature field, and the entire near-surface layer is occupied by the coldest (θ < −1.6 °C) and low-salinity (*S* < 33.6 PSU) Antarctic Surface Water of the high-latitude modification, which is called the Weddell Sea Surface Water (WSSW) in accordance with [2] (Figs. 2, *c* – *f*; 3, *b*, *c*).

Under the Antarctic Winter Water layer in the southern Scotia Sea, temperature increase is observed, and at the depths of 400–1000 m its intermediate maximum (θ ~ 1–1.2 °C) can be found, which is typical for the Circumpolar Deep Water Upper modification (UCDW) (Figs. 2, *a*; 3, *a*). Under the temperature maximum layer at the depths of 700–1400 m, weak salinity maximum (34.7–34.705 PSU) is observed, which characterizes the CDW Lower modification (LCDW) (Figs. 2, *b*; 3, *a*). The upper boundary of the UCDW layer qualitatively corresponds to the position of isopycnic line 28.05, the upper boundary of the LCDW layer corresponds qualitatively to the position of isopycnic line 28.1, which is consistent with the results of [18]. At the same time, the identification of two CDW modifications (Upper and Lower) in the southern Scotia Sea clarifies the results of this work, according to which the entire CDW layer is occupied by its Lower modification to the south of the ACC system. To the south of the South Scotia Ridge, over the deep slopes of the depths of the Philip Ridge and the Joinville shelf, temperature increase is observed, corresponding to the UCDW, which can be monitored almost to the bottom (Fig. 2, *a*).

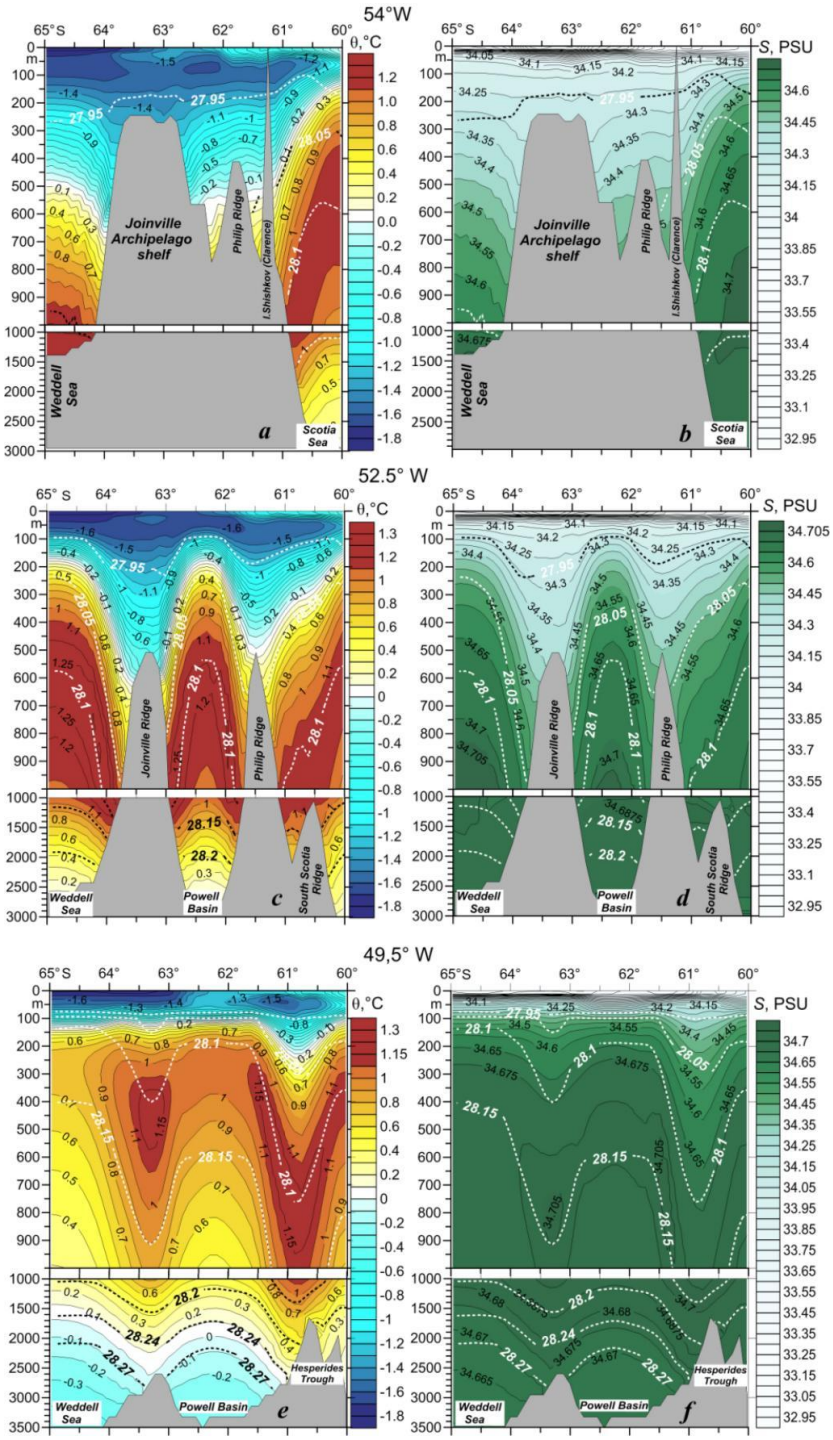

Fig. 2. Vertical distributions of long-term average potential temperature (*a*, *c*, *e*) and salinity (*b*, *d*, *f*) at sections along 54° W (*a*, *b*), 52.5° W (*c*, *d*) and 49.5° W (*e*, *f*). The dashed line shows neutral density γ^n isolines

Deeper than the LCDW layer in the southern Scotia Sea, monotonous temperature decrease is observed with uniform salinity distribution, corresponding to colder (θ < 0.5 °C) and less saline (*S* < 34.7 PSU) WSDW (Figs. 2, *a*, *b*; 3, *a*). According to the distribution of vectors of geostrophic currents (see Fig. 1, *b*) and the results shown in [2, 15–18], the WSDW penetrates into the Scotia Sea from the Weddell Sea and the Powell Basin through the deep-sea passages of the Philip and South Scotia Ridges. The upper WSDW boundary here corresponds approximately to the position of isopycnic line 28.15 (Figs. 2, *a*, *b*; 3, *a*).

To the east, in deep-water areas located between the Southern Scotia, Philip and Joinville Ridges (the Scotia Sea, the Powell Basin, the Weddell Sea), due to the cyclonic direction of the currents (see Fig. 1, *b*), a noticeable rise of the CDW layer is observed closer to the surface (Fig. 2, *c* – *f*).

In the central part of the Powell Basin and in the deep-sea part of the Weddell Sea, closer to the WSG center, the upper and lower boundaries of the UCDW and LCDW are located approximately 500–600 m higher than over the slopes of the depths, judging by the position of layers of intermediate temperature and salinity maxima and neutral density γ^n isopycnic lines 28.05, 28.1, and 28.15 (Figs. 2, *e*, *f*; 3, *c*). Due to the intense rise of colder waters, the intermediate temperature maximum weakens, the temperature in the UCDW layer decreases by approximately 0.2–0.3 °C (Fig. 2, *e*). It should be noted that in the Weddell Sea, in the lower part of the CDW layer, a weak maximum of salinity can be observed, which, in contrast to [2], makes it possible to divide the CDW layer into Upper and Lower modifications.

Under the CDW layer, deeper than 1500–2000 m, monotonous temperature decrease and uniform salinity distribution corresponding to the WSDW and WSBW can be observed (Fig. 2, *c* – *f*). There are no clearly expressed extrema on the long-term average θ,*S*-curves that would make it possible to separate these water masses (Fig. 3, *b*, *c*). According to [18], the WSBW layer is separated from the Weddell Sea deep water layer by the position of the isolines of neutral density γ^n > 28.24–28.27. This boundary is clearly visible in vertical sections of temperature and salinity passing over the deep-sea parts of the Powell Basin and the Weddell Sea, with the temperature and salinity values in the WSBW layer decreasing noticeably compared to their WSDW layer values, respectively, to −0.5…0.1 °C and 34.66–34.675 PSU (Fig. 2, *e*, *f*). We identify the end point on the θ,*S*-curves in these areas as the WSBW core, and the WSDW core is not clearly identified as an extremum (Fig. 3, *c*).

Over the shallow shelf of the Joinville Archipelago with depths less than 300 m, the long-term average vertical stratification of waters has its own characteristics. Here, the AAShW is characterized by weak subsurface temperature increase of approximately 0.1–0.2 °C in a layer of 20–30 m (Figs. 2, *a*; 3, *a*) and gradual salinity increase with depth (Fig. 2, *b*). Weak temperature inversion in the subsurface layer with a positive vertical salinity gradient in coastal shelf areas was noted earlier in [27]. It should be noted that the AAShW traces with the inversion of θ up to 0.15 °C in the subsurface layer of 15–25 m are observed over the slopes of the depths in the northwestern Weddell Sea (Fig. 3, *b*). To the south of 64° S, temperature and salinity increase monotonically with depth to the bottom (Fig. 2, *a*, *b*). At the same time, the distribution of isopycnic lines of neutral density γ^n shows that isopycnic line 28.05 is located at the depths of 950–1100 m, corresponding to the UCDW upper boundary.

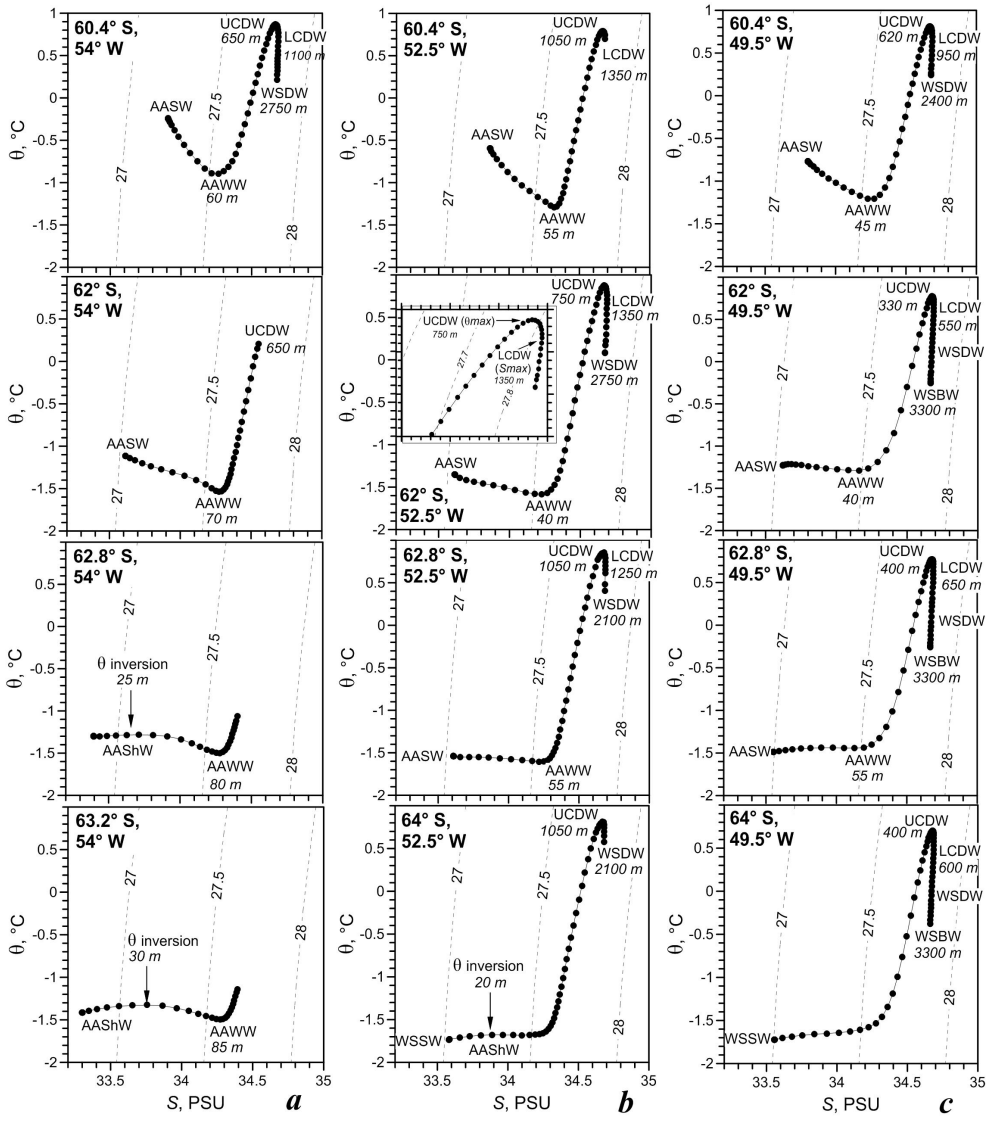

F i g . 3 . Examples of long-term average θ,*S*-curves in separate grid nodes located at 54° W (*a*), 52.5° W (*b*) and 49.5° W (*c*). The numbers next to the curves are the depths of the water mass cores (m). The dashed lines are isopycnic lines of conditional density σ_t. The inset shows an enlarged fragment of the θ,*S*-curve showing the presence of intermediate temperature and salinity maxima

The distributions of the thermohaline indices of the UCDW and LCDW cores, defined as intermediate maxima of temperature and salinity, respectively, and the depths of their occurrence (Fig. 4) illustrate clearly the qualitative connection of their spatial variability with the features of the bottom topography and the main elements of circulation. The minimum values of the UCDW θ-index are observed over the seaward edge of the shelves of the Joinville Archipelago and the Philip Ridge with the depths of less than 800 m, as well as in the Weddell Sea closer to the WSG center, where they make 0.4–0.5 °C and 0.5–0.7 °C, respectively. The UCDW core temperature decrease (1.05–1.1 °C) associated both with the cyclonic rise of waters and with the penetration of colder waters from the Weddell Sea (Fig. 1, *b*) is noted in the deep-sea part of the Powell Basin. In the southern Scotia Sea and over the slopes of the depths of the Jouinville Archipelago and Philip Ridge shelves with the depths of more than 1500 m, the θ-index values increase to 1.15–1.35 °C (Fig. 4, *a*). The range of spatial variability of the LCDW θ-index is

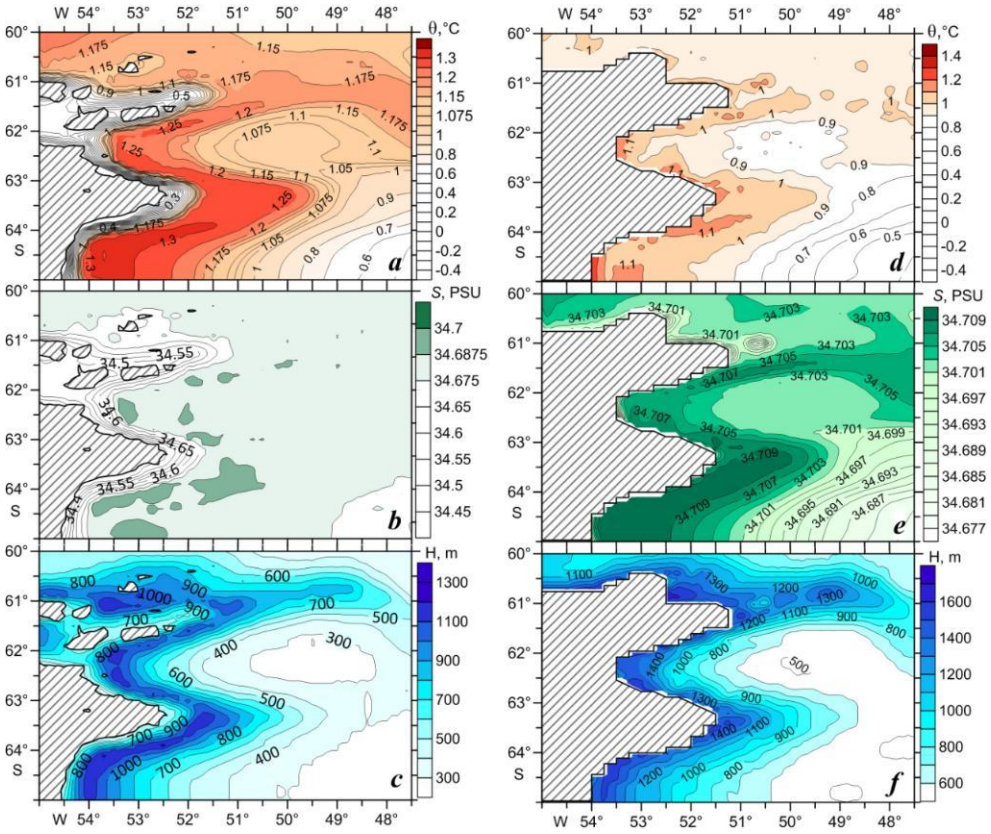

F i g . 4 . Spatial distributions of θ-indices (*a*, *d*), *S*-indices (*b*, *e*) and core depths *H* (*c*, *f*) of the Upper (*a*–*c*) and Lower (*d*–*f*) modifications of CDW. The areas, where UCDW and LCDW are absent, are shaded

significantly lower than that of the UCDW θ-index. At the same time, there is also a tendency towards a decrease in the values of the LCDW θ-index in the WSG area (0.5–0.7 °C) and in the central part of the Powell Basin (0.85–0.9 °C) and an increase over the slopes of the depths (to 1–1.1 °C) (Fig. 4, *d*).

The spatial variability of the UCDW *S*-index in most water area (in the Scotia and Weddell Seas, Powell Basin, Hesperides Trough) is small with its values varying within 34.675–34.69 PSU (Fig. 4, *b*). A significant decrease in the values of the UCDW *S*-index to 34.4–34.65 PSU, as well as its θ-index, is observed over the shelf edge with the depths less than 800 m. The low values of the UCDW θ,*S*-index here can be explained by the UCDW transformation due to its mixing with colder and fresher shelf water. Spatial changes in the values of the LCDW *S*-index (Fig. 4, *e*), which is its distinctive feature, are characterized by the same changes as in the UCDW θ-index. Decreased values of the UCDW *S*-index, as well as the UCDW θ-index, are observed in the WSG area (34.685–34.697 PSU) and in the central part of the Powell Basin (34.701–34.703 PSU), and increased ones (34.707–34.709 PSU) – over the slopes of the depths and in the southern Scotia Sea (Fig. 4, *e*).

The minimum depths of the UCDW core (less than 300 m) are observed in the areas of cyclonic gyres – in the central part of the Powell Basin and the Weddell Sea. Over the slopes of the depths, the UCDW core decreases to 1000–1300 m (Fig. 4, *c*). Similar spatial variability was revealed for the depth of the LCDW core. It is minimal (500–600 m) in the central part of the Powell Basin and the Weddell Sea and increases sharply (up to 1100–1500 m) over the slopes of the depths (Fig. 4, *f*). Qualitatively similar spatial features of the distribution of principal characteristics of the CDW Upper (θ-index) and Lower (*S*-index) modifications, as well as the depth of their cores, reflect the influence of the bottom topography and water circulation on the entire water layer occupied by the CDW.

Analysis of the distributions of intra-annual RMSD of potential temperature and salinity showed that the level of seasonal variability of these parameters varied noticeably over space (Fig. 5).

Intra-annual changes decrease significantly over the depth of 60–70 m in the temperature field (Fig. 5, *a* – *c*) and over the depth of 20–30 m in the salinity field (Fig. 5, *d* – *f*). The maximum level of intra-annual temperature variability is observed in the upper 20–30 m layer in the northern part of the water area (in the Scotia Sea, the Hesperides Trough, and over the South Scotia Ridge), where the θ RMSD values reach 1–1.6 °C (Fig. 5, *a* – *c*). The θ RMSD values decrease southward and amount to 0.6–0.8 °C in the Powell Basin (Fig. 5, *b*, *c*), 0.4–0.5 °C over the Joinville shelf (Fig. 5, *a*). The minimum level of intra-annual temperature variability is observed in the Weddell Sea, where the θ RMSD values do not exceed 0.2 °C (Fig. 5, *a* – *c*).

The spatial distribution of the intra-annual salinity RMSD differs significantly from the distribution of the temperature RMSD. The maximum *S* RMSD values are observed in the areas of intense ice formation and melting – over the Philip Ridge, the Joinville shelf and Ridge (0.5–0.8 PSU) (Fig. 5, *d*, *e*), as well as in the deep Weddell Sea (0.6–0.7 PSU) (Fig. 5, *f*).

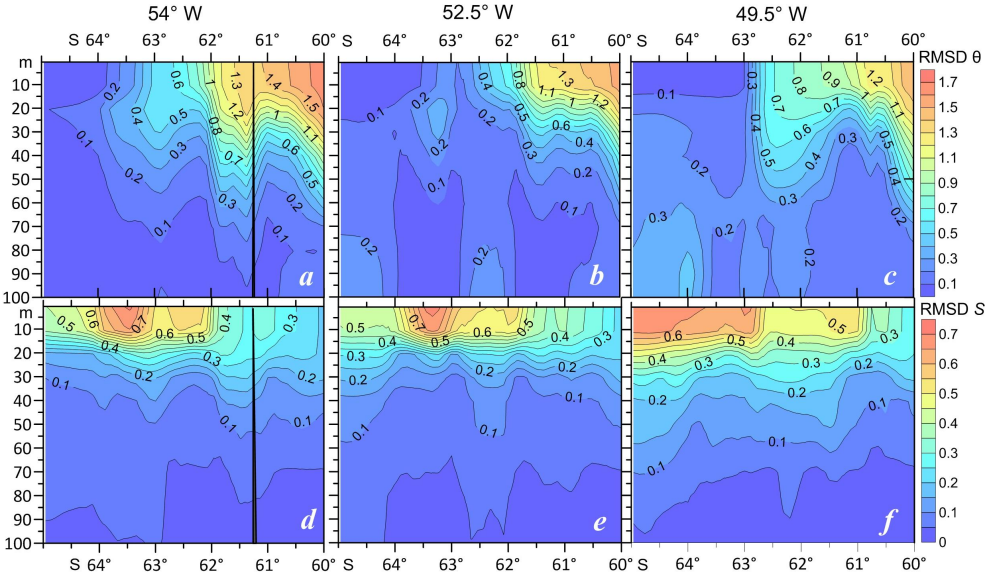

F i g . 5 . Vertical distributions of intra-annual RMSD of potential temperature (*a*–*c*) and salinity (*d*–*f*) along 54° W (*a*, *d*), 52.5° W (*b*, *e*) and 49.5° W (*c*, *f*). The dark band in Fig. 5, *a*, *d* is Shishkov Island

Over the slopes of the depths in the northwestern Weddell Sea and in the western part of the Powell Basin, the *S* RMSD values make 0.45–0.6 PSU (Fig. 5, *d*, *e*), and in the central deep-sea part of the Powell Basin they decrease to 0.4–0.5 PSU (Fig. 5, *f*). Minimum level of intra-annual salinity variability (*S* RMSD < 0.2–0.4 PSU) is observed in the areas of maximum intra-annual temperature variability – in the Scotia Sea and the Hesperides Trough (Fig. 5, *d* – *f*).

Spatial changes in the level of intra-annual variability of thermohaline parameters are reflected in climatic seasonal changes in θ,*S*-indices of water masses. Analysis of average monthly θ,*S*-curves showed that the greatest intra-annual changes in thermohaline indices characterized water masses of the upper 60–70 m ocean layer, in which the maximum seasonal variations of thermohaline fields were observed (Figs. 5; 6, *a*; 7). The maximum intra-annual changes in thermohaline indices are observed for the Antarctic Surface Water characterized by its Winter (AASWW) and Summer (AASSW) modifications (Fig. 6, *a*). The maximum seasonal changes in the ASW temperature index are observed in the southern Scotia Sea, where they reach almost 4 °C. In the Hesperides Trough, the θ-index changes make 3.5 °C. Over the Philip Ridge and in the northern and central parts of the Powell Basin, they decrease to 2–2.5 °C, and in its southern part – to 1–1.1 °C (Fig. 6, *b*). The AASW *S*-index intra-annual changes are maximum over the Philip Ridge and in the northern and southern parts of the Powell Basin, where they reach almost 1.9 PSU. In the Scotia Sea, the Hesperides Trough, and in the central part of the Powell Basin, the AASW *S*-index seasonal changes decrease to 0.8–1 PSU (Fig. 6, *c*).

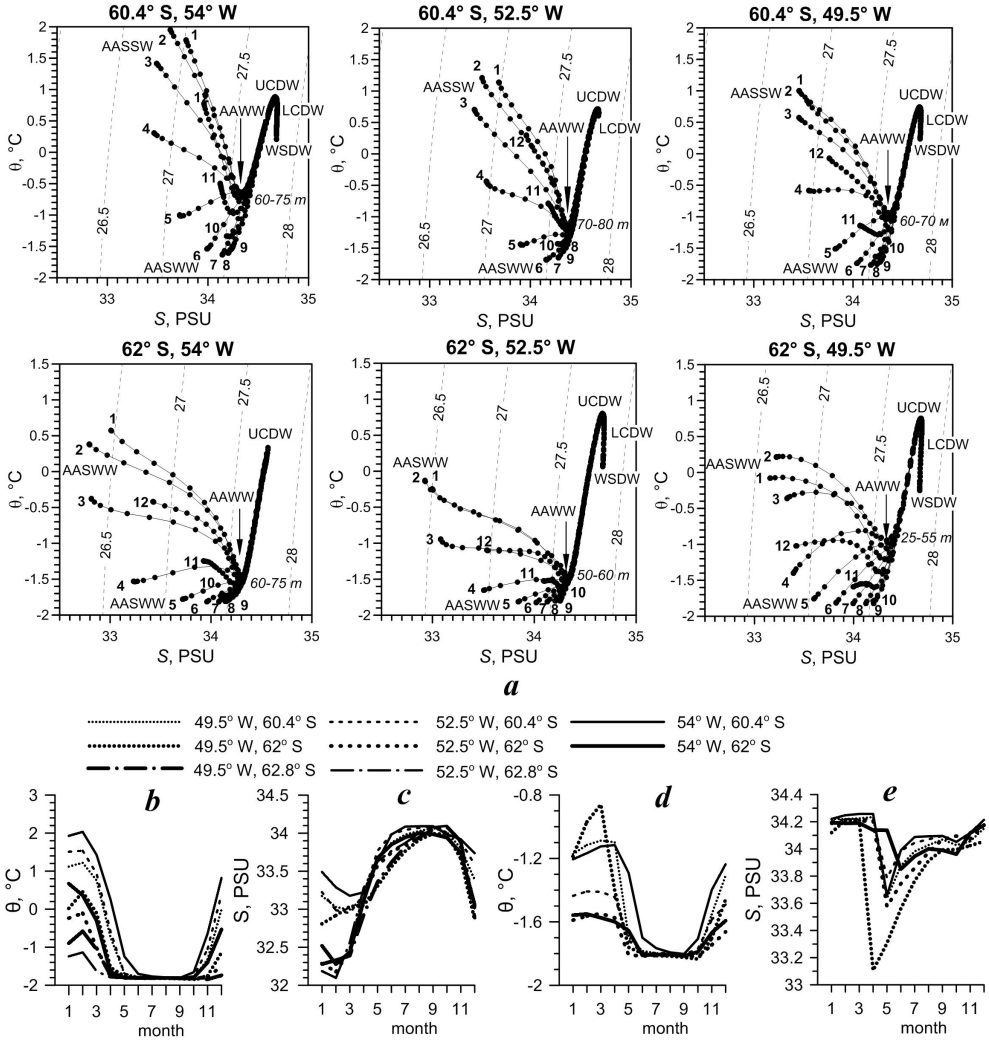

Fig. 6. Examples of monthly average θ,*S*-curves in separate grid nodes (*a*) and graphs of the intra-annual cycle of the θ-index (*b*, *d*) and *S*-index (*c*, *e*) of the ASW (*b*, *c*) and AWW (*d*, *e*). The numbers at the curves in Figs. 6, *a* – months and depths of the AWW core (m)

It should be noted that the value of the amplitude of intra-annual changes in the AASW θ,*S*-indices and its spatial variability depend mainly on the changes in the θ,*S*-indices of the AASW Summer modification. Throughout the entire water area, there are almost no changes in the values of the AASW Winter modification θ,*S*-indices, which amount to −1.8…−1.6 °C and 34–34.1 PSU in the period from May to October (Fig. 6, *b*, *c*). The values of the AASW Summer modification θ-index in January–March make 1.2–2 °C in the Scotia Sea and the Hesperides Trough, 0.6–0.8 °C over the Philip Ridge and decrease to −0.2…0.4 °C

in the northern and central parts of the Powell Basin and to −1.1…−0.6 °C in its southern part (Fig. 6, *b*). The values of the AASSW *S*-index make 32.1–32.5 PSU over the Philip Ridge in the northern and southern parts of the Powell Basin, 32.8–33 PSU in its central part, 33.2–33.5 PSU in the Scotia Sea and the Hesperides Trough (Fig. 6, *c*).

In the Weddell Sea, the temperature index of the AASW high-latitude modification – WSSW – varies throughout the year from −1.85...−1.8 °C in winter to −1.2...−1.1 °C in summer. The WSSW *S*-index intra-annual changes make almost 1.8 PSU (from 34.2–34.3 PSU in winter to 32.5–32.8 PSU in summer) (Fig. 7).

The AAWW can be observed in the subsurface layer throughout the year in the southern Scotia Sea, in the Hesperides Trough, over the Philip Ridge, in the northern and central parts of the Powell Basin (Fig. 6, *a*). Intra-annual changes in the AAWW θ,*S*-indices are maximum in the central part of the Powell Basin (up to 1 °C and 1.1 PSU), where the AAWW core is located closer to the surface in a 25–55 m layer due to the rise of water in the center of the cyclonic circulation. Minimum changes in the AAWW θ,*S*-indices, not exceeding 0.4 °C and 0.3 PSU, are observed in the Scotia Sea, the Hesperides Trough, and over the Philip Ridge, where the AAWW core deepens to 60–85 m (Fig. 6, *d*, *e*).

In the southern part of the studied water area, the AAWW is observed only for a part of the year due to the intense convection during the cold period (Fig. 7). Over the Joinville shelf, the AAWW is observed from September–November to May–June, in the southern part of the Powell Basin – from November–December to April, in the Weddell Sea – from December to March–April. In these areas, the AAWW θ,*S*-indices show poor spatiotemporal variability and amount to −1.8…−1.4 °C and 34.1–34.2 PSU, respectively. A slight increase in the AAWW θ-index (up to −1.4…−1.1 °C) is noted in the southern part of the Powell Basin (Fig. 7).

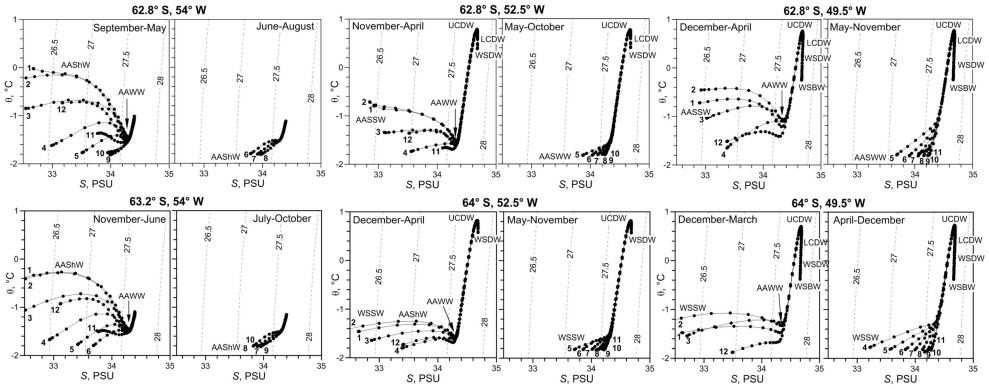

Fig. 7. Examples of monthly average θ,*S*-curves in separate grid nodes. The numbers at the curves are months.

The AAShW, like the AASW, is characterized by significant changes in thermohaline indices. Over the Joinville shelf, intra-annual changes in the AAShW θ-index reach 1.6–1.8 °C (from −1.8 °C in winter to −0.2…0 °C in summer), changes in the *S*-index amount to almost 1.5 PSU (from 33.9–34 to 32.5–32.6 PSU in summer) (Fig. 7).

Conclusions

Based on the *ECMWF ORAS*5 reanalysis data for the period from 1958 to 2021, the long-term average structure and climatic intra-annual variability of water mass characteristics in the Powell Basin and adjacent water areas are analyzed. The AASW and its colder and less saline modification, the Weddell Sea surface water, were identified as well as the AAShW, AAWW, CDW, WSDW, and WSBW. It is shown that the AAShW is observed not only over the shallow shelf of the Joinville Archipelago, but also over the continental slope in the northwestern Weddell Sea. It is revealed that in deep water areas, the CDW layer is divided into Upper and Lower modifications characterized by intermediate temperature and salinity maximums, respectively. The WSDW and WSBW do not appear in the form of separate extrema on the long-term average θ,*S*-curves.

It is shown that due to the rise of water in the center of the cyclonic gyre in the Powell Basin, the Antarctic Winter Water core is located closer to the surface in a layer of 25–55 m. In the Scotia Sea, the Hesperides Trough, and over the Philip Ridge, it deepens to 60–85 m. The minimum UCDW and LCDW core depths (250–300 m and 500–600 m, respectively) are also observed in the central part of the Powell Basin and in the Weddell Sea, closer to the WSG. The maximum UCDW and LCDW core depths (1000–1300 m and 1100–1500 m, respectively) are observed over the slopes of the depths of the Joinville shelf and the South Scotia, Philip, and Joinville Ridges.

An increase in the values of the UCDW θ-index and the LCDW *S*-index is revealed (up to 1.15–1.35 °C and 34.707–34.709 PSU, respectively) in the southern Scotia Sea and over the slopes of the depths of the shelf of the Joinville Archipelago and the Philip Ridge with the depths of more than 1500 m. A decrease in temperature in the UCDW core and salinity in the LCDW core is also observed in the Weddell Sea (0.5–1 °C and 34.685–34.699 PSU) and in the deep-sea part of the Powell Basin (1.05–1.1 °C and 34.701–34.703 PSU). The minimum values of the UCDW θ-index (0.4–0.7 °C) are observed over the edge of the shelves of the Joinville Archipelago and the Philip Ridge with the depths less than 800 m.

The maximum intra-annual changes in thermohaline indices characterize the AASW with its Winter and Summer modifications. Seasonal changes in the AASW θ-index are maximum in the southern Scotia Sea, where they reach almost 4 °C, and in the Hesperides Trough they are 3.5 °C, over the Philip Ridge and in the northern and central parts of the Powell Basin they decrease to 2–2.5 °C, and in its southern part – to 1–1.1 °C. Intra-annual changes in the AASW *S*-index are maximum over the Philip Ridge and in the northern and southern parts of the Powell Basin, where they reach almost 1.9 PSU. In the Scotia Sea, the Hesperides Trough, and in the central part of the Powell Basin, seasonal changes in the AASW *S*-index decrease to 0.8–1 PSU.

The WSSW is characterized by weak changes in the θ-index throughout the year (from −1.85…−1.8 °C in winter to −1.2…−1.1 °C in summer), while changes in its *S*-index reach almost 1.8 PSU (from 34.2–34.3 PSU in winter to 32.5 –32.8 PSU in summer).

The AAShW, like the AASW, is characterized by significant changes in thermohaline indices. Intra-annual changes in the AAShW θ-index reach 1.6–1.8 °C (from −1.8 °C in winter to −0.2…0 °C in summer), changes in the *S*-index amount to almost 1.5 PSU (from 33.9–34 to 32.5–32.6 PSU in summer).

Intra-annual changes in the AAWW θ,*S*-indices are maximum in the central part of the Powell Basin (up to 1 °C and 1.1 PSU), minimal (up to 0.4 °C and 0.3 PSU) in the Scotia Sea, the Hesperides Trough, and above the Philip Ridge. In the southern part of the water area, the AAWW is not visible in all months. Over the Joinville shelf, the AAWW is observed from September–November to May–June, in the southern part of the Powell Basin – from November–December to April, in the Weddell Sea – from December to March–April. In these areas, the AAWW θ,*S*-indices vary slightly both in space and time.

REFERENCES

1. Dubravin, V.F., 2001. [*Surface Water Masses and the Formation of Zones of Biological Productivity of the Atlantic Ocean*]. Saint Petersburg: Gidrometeoizdat, 115 p. (in Russian).
2. Maslennikov, V.V., 2003. *Climatic Variability and Marine Ecosystem of the Antarctic*. Moscow: VNIRO Publishing, 295 p. (in Russian).
3. Shulgovsky, K.E., 2005. [*Large-Scale Variability of Oceanological Conditions in the Western Part of the Atlantic Sector of the Antarctic and its Influence on the Distribution of Krill*]. Kaliningrad: AtlantNIRO, 148 p. (in Russian).
4. Venables, H., Meredith, M.P., Atkinson, A. and Ward, P., 2012. Fronts and Habitat Zones in the Scotia Sea. *Deep-Sea Research Part II: Topical Studies in Oceanography*, 59–60, pp. 14–24. doi:10.1016/j.dsr2.2011.08.012
5. Arzhanova, N.V. and Artamonova, K.V., 2014. Hydrochemical Structure of Water Masses in Areas of the Antarctic Krill (*Euphausia superba Dana*) Fisheries. *Trudy VNIRO*, 152, pp. 118–132 (in Russian).
6. Lohmann, R. and Belkin, I.M., 2014. Organic Pollutants and Ocean Fronts across the Atlantic Ocean: A Review. *Progress in Oceanography*, 128, pp. 172–184. doi:10.1016/j.pocean.2014.08.013
7. Chapman, C.C., Lea, M.-A., Meyer, A., Sallée, J.-B. and Hindell, M., 2020. Defining Southern Ocean Fronts and their Influence on Biological and Physical Processes in a Changing Climate. *Nature Climate Change*, 10, pp. 209–219. doi:10.1038/s41558-020-0705-4
8. Siegel, V. and Watkins, J.L., 2016. *Distribution, Biomass and Demography of Antarctic Krill, Euphausia superba*. In: V. Siegel, ed., 2016. Biology and Ecology of Antarctic Krill. Cham: Springer, pp. 21–100. doi:10.1007/978-3-319-29279-3_2
9. Spiridonov, V.A., Zalota, A.K., Yakovenko, V.A. and Gorbatenko, K.M., 2020. Composition of Population and Transport of Juveniles of Antarctic Krill in Powell Basin Region (Northwestern Weddell Sea) in January 2020. *Trudy VNIRO*, 181, pp. 33–51. doi:10.36038/2307-3497-2020-181-33-51 (in Russian).

10. Morozov, E.G., Spiridonov, V.A., Molodtsova, T.N., Frey, D.I., Demidova, T.A. and Flint, M.V., 2020. Investigations of the Ecosystem in the Atlantic Sector of Antarctica (Cruise 79 of the R/V Akademik Mstislav Keldysh). *Oceanology*, 60(5), pp. 721–723. https://doi.org/10.1134/S0001437020050161
11. Orsi, A.H., Nowlin Jr., W.D. and Whitworth III, Th., 1993. On the Circulation and Stratification of the Weddell Gyre. *Deep-Sea Research Part I: Oceanographic Research Papers*, 40(1), pp. 169–203. doi:10.1016/0967-0637(93)90060-G
12. Fahrbach, E., Rohardt, G., Scheele, N., Schröder, M., Strass, V. and Wisotzki, A., 1995. Formation and Discharge of Deep and Bottom Water in the Northwestern Weddell Sea. *Journal of Marine Research*, 53(4), pp. 515–538. doi:10.1357/0022240953213089
13. Artamonov, Yu.V., Popov, Yu.I. and Trotsenko, B.G., 1997. Water Masses in Antarctic Sector of South-Western Atlantic in February-April 1997. In: UAC, 1997. *UAC Bulletin*. Kyiv. Iss. 1, pp. 125–131 (in Russian).
14. Naveira Garabato, A.C., McDonagh, E.L., Stevens, D.P., Heywood, K.J. and Sanders, R.J., 2002. On the Export of Antarctic Bottom Water from the Weddell Sea. *Deep-Sea Research Part II: Topical Studies in Oceanography*, 49(21), pp. 4715–4742. https://doi.org/10.1016/S0967-0645(02)00156-X
15. Franco, B.C., Mata, M.M., Piola, A.R. and Garcia, C.A.E., 2007. Northwestern Weddell Sea Deep Outflow into the Scotia Sea during the Austral Summers of 2000 and 2001 Estimated by Inverse Methods. *Deep Sea Research Part I: Oceanographic Research Papers*, 54(10), pp. 1815–1840. doi:10.1016/j.dsr.2007.06.003
16. Thompson, A.F. and Heywood, K.J., 2008. Frontal Structure and Transport in the Northwestern Weddell Sea. *Deep Sea Research Part I: Oceanographic Research Papers*, 55(10), pp. 1229–1251. doi:10.1016/j.dsr.2008.06.001
17. Tarakanov, R.Yu., 2009. Antarctic Bottom Water in the Scotia Sea and the Drake Passage. *Oceanology*, 49(5), pp. 607–621. doi:10.1134/S0001437009050026
18. Palmer, M., Gomis, D., del Mar Flexas, M., Jordà, G., Jullion, L., Tsubouchi, T. and Naveira Garabato, A.C., 2012. Water Mass Pathways and Transports over the South Scotia Ridge West of 50°W. *Deep Sea Research Part I: Oceanographic Research Papers*, 59, pp. 8–24. doi:10.1016/j.dsr.2011.10.005
19. Morozov, E.G., Frey, D.I., Polukhin, A.A., Krechik, V.A., Artemiev, V.A., Gavrikov, A.V., Kasian, V.V., Sapozhnikov, F.V., Gordeeva, N.V. and Kobylyansky, S.G., 2020. Mesoscale Variability of the Ocean in the Northern Part of the Weddell Sea. *Oceanology*, 60(5), pp. 573–588. https://doi.org/10.1134/S0001437020050173
20. Fedotova, A.A. and Stepanova, S.V., 2021. Water Mass Transformation in the Powell Basin. In: E. G. Morozov, M. V. Flint and V. A. Spiridonov, eds., 2021. *Antarctic Peninsula Region of the Southern Ocean*. Cham: Springer, pp. 115–129. doi:10.1007/978-3-030-78927-5_8
21. Mukhametyanov, R.Z. and Frey, D.I., 2021. [Mesoscale Variability of the Characteristics of Water Masses and Currents in the Northern Weddell Sea (Powell Basin)]. In: IO RAS, 2021. *Complex Investigations of the World Ocean.* Proceedings of the VI Russian Scientific Conference of Young Scientists, Moscow, April 18–24, 2021. Moscow: Shirshov Institute of Oceanology RAS, p. 139. doi:10.29006/978-5-6045110-3-9 (in Russian).
22. Orsi, A.H., Whitworth III, Th. and Nowlin Jr., W.D., 1995. On the Meridional Extent and Fronts of the Antarctic Circumpolar Current. *Deep Sea Research Part I: Oceanographic Research Papers*, 42(5), pp. 641–673. doi:10.1016/0967-0637(95)00021-W

23. Morozov, E.G., Flint, M.V., Orlov, A.M., Frey, D.I., Molodtsova, T.N., Krechik, V.A., Latushkin, A.A., Salyuk, P.A., Murzina, S. A. [et al.], 2022. Oceanographic and Ecosystem Studies in the Atlantic Sector of Antarctica (Cruise 87 of the Research Vessel Akademik Mstislav Keldysh). *Oceanology*, 62(5), pp. 721–723. https://doi.org/10.1134/S0001437022050150
24. Zuo, H., Balmaseda, M.A., Tietsche, S., Mogensen, K. and Mayer, M., 2019. The ECMWF Operational Ensemble Reanalysis-Analysis System for Ocean and Sea Ice: A Description of the System and Assessment. *Ocean Science*, 15(3), pp. 779–808. doi:10.5194/os-15-779-2019
25. Dobrovolskii, A.D., 1961. On the Estimation of Water Masses. *Oceanology*, 1(1). pp. 12–24 (in Russian).
26. Jackett, D.R. and McDougall, T.J., 1997. A Neutral Density Variable for the World's Oceans. *Journal of Physical Oceanography*, 27(2), pp. 237–263. doi:10.1175/1520-0485(1997)027<0237:ANDVFT>2.0.CO;2
27. Artamonov, Yu.V., Bulgakov, N.P., Lomakin, P.D. and Skripaleva, E.A., 2004. Vertical Thermohaline Structure, Water Masses, and Large-Scale Fronts in the South-West Atlantic and Neighboring Antarctic Water Areas. *Physical Oceanography*, 14(3), pp. 161–172. https://doi.org/10.1023/B:POCE.0000048898.31072.cc

Submitted 29.04.2023; accepted after review 18.05.2023;
revised 28.06.2023; published 25.09.2023

About the authors:

Yuri V. Artamonov, Leading Research Associate, Marine Hydrophysical Institute of RAS (2 Kapitanskaya St., Sevastopol, 299011, Russian Federation), Dr.Sci. (Geogr.), **ResearcherID: AAC-6651-2020**, *artam-ant@yandex.ru*

Elena A. Skripaleva, Senior Research Associate, Marine Hydrophysical Institute of RAS (2 Kapitanskaya St., Sevastopol, 299011, Russian Federation), Ph.D. (Geogr.), **ResearcherID: AAC-6648-2020,** *sea-ant@yandex.ru*

Nikolay V. Nikolskii, Junior Research Associate, Marine Hydrophysical Institute of RAS (2 Kapitanskaya St., Sevastopol, 299011, Russian Federation), **ResearcherID: AAC-7723-2020**, *nikolsky.geo@gmail.com*

Contribution of the authors:

Yuri V. Artamonov – general scientific supervision of the study, statement of the study aims and objectives, method development, qualitative analysis of the results and their interpretation, discussion of the work results, formulation of conclusions

Elena A. Skripaleva – review of literature on the study problem, qualitative analysis of the results and their interpretation, processing and description of the study results, discussion of the work results, formulation of conclusions, preparation of the manuscript, text refinement

Nikolay V. Nikolskii – development and debugging of computer programmes for data processing, algorithm programming, graph plotting, participation in discussion of the article materials

All the authors have read and approved the final manuscript.